



PII: S1464-1909(99)00088-X

On the Control Volume Modelling of Near-Surface Soil Drying

S. Orlandini

Dipartimento di Ingegneria delle Strutture, dei Trasporti, delle Acque, del Rilevamento, del Territorio, Università degli Studi di Bologna, Viale Risorgimento 2, I-40136 Bologna, Italy
E-mail: stefano@idraulica.ing.unibo.it

Received 12 September 1998; accepted 30 November 1998

Abstract. The problem of simulating the topsoil water dynamics in response to atmospheric evaporative events is considered in the present paper. It is emphasised how the assumption that soil moisture profiles approximately preserve similarity during simultaneous atmospheric drying and gravity drainage may be required in order to incorporate the effects of deep soil layers in the near-surface soil control volume hydrologic modelling. The reliability of the proposed formulation is evaluated with rates of evaporation calculated from measurements of the Bowen ratio and soil moisture data obtained from time domain reflectometry measurements for a bare soil field in the Zwalmbeek catchment (Belgium).

© 1999 Elsevier Science Ltd. All rights reserved.

1 Introduction

Simulations of the land surface response to atmospheric forcing during storm-interstorm sequences are required in catchment scale hydrology, agricultural engineering, and large-scale meteorology. The problem of the simulation of local scale land surface dynamics during evaporative events has been dealt with in various papers. Detailed numerical solutions of the heat and mass transport equations have been tested under laboratory and field conditions (e.g., van Bavel and Hillel, 1976; Sophocleous, 1979; Milly, 1982; Camillo et al., 1983; Higuchi, 1984; Passerat de Silans et al., 1989; Witono and Bruckler, 1989). These studies have shown that detailed heat and mass flow models coupled with accurate soil surface energy and radiation balances usually gives satisfactory results after a calibration phase. However, the simulation of the topsoil water dynamics in detailed numerical models can incur prohibitive computational expenses, owing to rapid response of this zone to atmospheric forcing, which constrains such models to small grid and time steps. This motivates a need for simplifying the description of the land surface moisture dynamics through the introduction of soil-vegetation-atmosphere transfer schemes (SVATSs).

A number of laboratory studies such as those by Richards et al. (1956), Youngs (1960), Gardner (1962), Gardner and Hillel (1962), Prill et al. (1965), and Gardner and Gardner (1969), suggest that it may be possible to describe the relation of evaporation and drainage to soil water content by relatively simple though somewhat approximate expressions based upon the theory of water flow in porous media. A variety of simplified models were developed for local scale investigations (e.g., Black et al., 1969; Gardner, 1973, 1974; Milly, 1986), catchment hydrologic simulations (e.g., Famiglietti and Wood, 1994; Wigmosta et al., 1994; Flerchinger et al., 1996), and numerical weather predictions (e.g., Sellers et al., 1986; Dickinson et al., 1993). In the formulation presented in this paper special emphasis has been given to the control volume description of near-surface soil drying and the assumption of soil moisture profile similarity introduced by Salvucci (1997) is used to incorporate the effects of deep soil layers on the land surface dynamics. The linkage of the scheme developed in the present paper to that developed in Orlandini et al. (1996) for the description of land surface dynamics during storm events provides a complete model for land surface hydrologic simulations on a continuous-time basis. The reliability of the model is evaluated with rates of evaporation calculated from measurements of the Bowen ratio and soil moisture data obtained from time domain reflectometry (TDR) measurements. Experiments were carried out for three periods of several days each at Ghent, Belgium, over a bare soil field in the summer of 1994.

2 Model formulation

The theoretical basis on which the model is built are the Penman-Monteith formulation, for the evaluation of the potential flux across the land surface in response to the atmospheric evaporative demand, and the theory of water flow in unsaturated-saturated soil domains, for the description of the soil profile response to land surface drying and gravitational drainage. The Penman-Monteith equation can be written in

Correspondence to: S. Orlandini

the form

$$\rho_w L_e e = \frac{\Delta (Q_n - Q_g) + \rho_a c_p [\epsilon_s(T) - \epsilon]/r_a}{\Delta + \gamma (1 + r_s/r_a)}, \quad (1)$$

where ρ_w is the density of water, L_e is the latent heat of vapourisation per unit mass of water, e is the evaporation rate, Δ is the rate of change of saturated vapour pressure with temperature, Q_n is the net radiation flux density, Q_g is the soil heat flux density, ρ_a is the density of air, c_p is the specific heat of air at constant pressure, $\epsilon_s(T)$ is the saturated vapour pressure at screen temperature T , ϵ is the vapour pressure at screen height, r_a is the aerodynamic resistance to water vapour transfer, γ is the psychrometer constant, p_a is the ambient atmospheric pressure at the ground surface, and r_s is the surface resistance to water vapour transfer.

The water motion in the unsaturated soil domain is assumed to obey the classical Richards equation, which can be written in its one-dimensional form with pressure head as the dependent variable as

$$\sigma(\psi) \frac{\partial \psi}{\partial t} = \frac{\partial}{\partial z} \left[K_s K_r(\psi) \frac{\partial(z + \psi)}{\partial z} \right], \quad (2)$$

where $\sigma(\psi) = d\theta/d\psi$ is the specific moisture capacity, t is time, z is the vertical coordinate (positive upward), and the hydraulic conductivity is expressed as a product of the conductivity at saturation, K_s , and the relative conductivity, $K_r(\psi)$. This equation is easily obtained by incorporating the expression of the vertical Darcian flux for saturated-unsaturated domain,

$$q_z = -K_s K_r(\psi) \frac{\partial(z + \psi)}{\partial z}, \quad (3)$$

into the continuity equation $\partial\theta/\partial t + \partial q_z/\partial z = 0$. The constitutive relationships introduced by Brooks and Corey (1966) are used to describe the nonlinear dependencies of θ , K_r , and σ on ψ . Vapour fluxes and thermal effects are neglected in Eq. (2). Philip and de Vries (1957) noted that during soil limited evaporation the sites of phase change occur lower in the soil, leaving a dry layer in which the dominant moisture transport mechanism is vapour flow along moisture and temperature gradients. At first glance the presence of this layer may appear to invalidate the application of methods based on liquid transport. However, the evaporation rate can still be estimated by modelling the liquid flow regime beneath this layer, so long as vapour can be transported through the dry layer at a rate greater than or equal to the rate of the liquid flow below. The applicability of simplified single-phase isothermal descriptions depends not on the presence or absence of a dry layer but rather on which process is limiting (Salvucci, 1997). The work presented here assumes that the evaporation rate is ultimately limited by liquid flow and thus that a simple single-phase isothermal process model description is adequate.

The essential parameters of the formulations mentioned above are incorporated into the SVATS sketched in Fig. 1. Two layers of different depth, Z_{up} and Z_{low} , are used to describe the highly dynamical water flux partitioning at the land

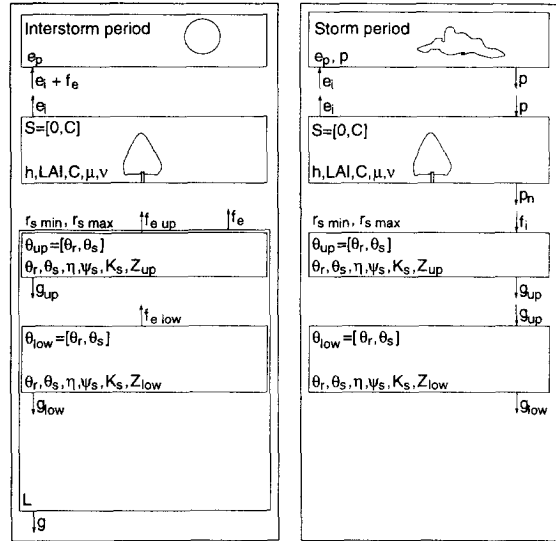


Fig. 1. Conceptualisation of the soil-vegetation-atmosphere continuum. Notations are: S , canopy storage; C , canopy storage capacity; h , canopy height; LAI , leaf area index; μ and ν , coefficients of the canopy storage-outflow relationships; $r_{s \min}$ and $r_{s \max}$, minimum and maximum values of surface resistance to water vapour transfer, respectively; θ , volumetric water content; θ_r and θ_s , residual and saturated volumetric soil water contents; η , pore-size distribution index; ψ_s , saturated soil matrix potential; K_s , saturated hydraulic conductivity; Z , soil layer depth; L , drying front depth; e_p , potential evaporation; p , gross precipitation; p_n , ground level precipitation; e_i , evaporation from the wet canopy; f_i and f_e , infiltration and exfiltration; g , drainage. Subscripts "up" and "low" indicate the upper and lower soil layer, respectively.

surface and the quasi-steady dynamics of the lower transmission zone, respectively (see Orlandini et al., 1996). Actual evapotranspiration is considered as a phenomenon associated with the soil and canopy moisture depletion responses to atmospheric potential demand. It is assumed that the atmospheric evaporative demand e_p is obtained by Eq. (1) with $r_s = 0$, and e_p is set to zero at night. Actual evaporation from wet canopy and soil is dynamically expressed as a function of e_p and the moisture status of each subsystem. If the atmospheric evaporative demand is not completely satisfied by the wet canopy, the residual rate acts as forcing of the soil-vegetation system and the water flux released by this system is limited by the surface resistance to vapour transfer r_s in Eq. (1) and by the exfiltration capacity of the unsaturated soil profile (soil limited evaporation). For bare soil simulations (such as that reported in the present paper) the simplified conceptualisation of the vegetation cover described in the next section is used to reproduce the aerodynamic and surface resistances to water vapour diffusion as well as the storage capacity produced by the bare soil at land surface. Dynamically, the model computes a series of steady state flux densities over short time intervals and recalculates storages at the end of each interval for use in the next interval.

2.1 Vegetation cover water balance

The water balance of the vegetation cover is expressed by the continuity equation

$$\frac{dS}{dt} = p - e_i - p_n, \quad (4)$$

where S is the actual water content of the cover, t is time, p is the gross precipitation above the canopy, e_i is the actual evaporation from the cover, and p_n is the ground level precipitation. On the basis of the works by Rutter and Morton (1977) and Massman (1980), ground level precipitation and actual evaporation from the wet cover are expressed through the storage-outflow relationships $e_i = e_p (S/C)^\mu$ and $p_n = p (S/C)^\nu$, respectively, where C is the potential retention of the cover, e_p is the wet surface potential evaporation, μ and ν are parameters characteristic of the vegetation cover. Equation (4) is solved numerically during storm and interstorm events by applying a simple explicit Euler scheme (see Orlandini, 1998).

2.2 Soil water balance

Data such as that of Prill et al. (1965) (obtained from laboratory studies of drainage from various sands) and Richards et al. (1956) (for drainage in the field) demonstrated that the soil matrix gradient term in the flow equation (3) is relatively small during a large fraction of the drainage process. In addition, it was observed that water drains almost equally from all layers above the initial wetting depth in a uniform profile. However, this evidence is not reproduced by simply neglecting the soil matrix gradient term in Eq. (3) as reported in many published formulations (e.g., Famiglietti and Wood, 1994; Wigmosta et al., 1994), as this assumption leads to excessive control volume outflows and premature control volume emptying. In the proposed formulation the lack in the knowledge of the soil moisture profile is filled with the assumption of geometric similarity of the vertical soil moisture profile introduced by Salvucci (1997), that is

$$\Theta(z, t) = \begin{cases} \Gamma[z/L(t)] & \text{if } -z < L \\ \Theta_i & \text{if } -z \geq L \end{cases}, \quad (5)$$

where $\Theta = (\theta - \theta_r)/(\theta_s - \theta_r)$ is the degree of soil saturation, $\Gamma(\cdot)$ is some (undetermined) function describing the shape of the drying profile, $L(t)$ is the scaling length of the profile and may be thought of approximately as a penetration depth of the drying front, and Θ_i is the (uniform) initial condition of soil saturation. As noted in Salvucci (1997), "Eq. (5) is not meant to imply that the drying front is sharp (as in the interpretation of Green and Ampt (1911) wetting fronts) but only that the profile preserves geometric similarity." This assumption is shown by Salvucci (1997) to be reasonable through comparison with a numerical solution of the Richards equation (2) for homogeneous soils under a wide range of conditions.

With the above similarity assumption the exfiltration capacity of the drying profile can be expressed through the time

compression approximation (TCA) concept as

$$f_{e*} = \frac{S_e^2}{2(F_e + G)}, \quad (6)$$

where S_e is the desorptivity, F_e is the cumulative exfiltration depth at the land surface in response to atmospheric (variable) drying, and G is the cumulative drainage depth at the drying front ($z = -L$) in response to gravity forces (Salvucci, 1997). The desorptivity S_e is evaluated on the basis of the soil hydraulic properties and initial (uniform) moisture content Θ_i , as given by Eagleson (1978). The initial condition of soil saturation Θ_i is expressed by

$$\Theta_i = \frac{Z_{up}}{Z_{up} + Z_{low}} \Theta_{up i} + \frac{Z_{low}}{Z_{up} + Z_{low}} \Theta_{low i}, \quad (7)$$

where $\Theta_{up i}$ and $\Theta_{low i}$ are the average initial soil moisture saturations of the upper and lower layer, respectively. The land surface boundary condition during interstorm events is assumed to be

$$\Theta_0 = 0. \quad (8)$$

The actual exfiltration flux at the land surface may be expressed as

$$f_e = \min(e_r, f_{e*}), \quad (9)$$

where e_r is the residual atmospheric evaporative demand and f_{e*} is the exfiltration capacity. Following Wigmosta et al. (1994), e_r is given by

$$e_r = (e_p - e_i) \frac{\Delta + \gamma}{\Delta + \gamma(1 + r_s/r_a)}, \quad (10)$$

where the control of land surface drying is incorporated by varying the surface resistance to water vapour transfer r_s with the upper layer moisture status Θ_{up} as proposed by Mahfouf and Noilhan (1991) and further investigated by Daamen and Simmonds (1996), that is

$$r_s = A \exp(B \Theta_{up}), \quad (11)$$

where $A = r_{s \max}$ and $B = -\ln(r_{s \max}/r_{s \min})$.

The gravity flux at the drying front ($z = -L$) may be expressed on the basis of Eq. (3), where the Brooks and Corey (1966) relationships are incorporated to estimate the unsaturated conductivity and the soil matrix gradient is neglected, that is

$$g = K_s \Theta_i^{(2+3\eta)/\eta}, \quad (12)$$

where Θ_i is the initial soil moisture saturation along the unsaturated profile as given by Eq. (7), and η is the pore-size distribution index introduced in Brooks and Corey (1966).

Water balances of the upper and lower soil layers are carried out by scaling the exfiltration and the drainage fluxes as obtained from the above TCA calculation. For the upper soil layer one can write

$$Z_{up} \frac{d\theta_{up}}{dt} = -f_{e \ up} - g_{up}, \quad (13)$$

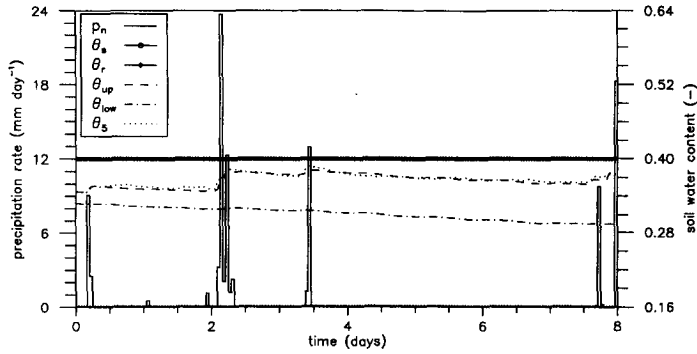


Fig. 2. Comparison between time series of computed average moisture contents of the upper soil layer, θ_{up} , and TDR soil moisture measurements at 5 cm depth, θ_5 .

Table 1. SVAT Simulation Parameters

Parameter	Value
h , m	0.10
LAI	1.00
C , mm	0.10
μ	0.15
ν	3.00
$r_{s \min}$, $m^{-1} s$	24
$r_{s \max}$, $m^{-1} s$	700
θ_r	0.16
θ_s	0.40
η	0.675
ψ_s , m	-0.98
K_s , $mm \text{ day}^{-1}$	57.0
Z_{up} , m	0.10
Z_{low} , m	0.60

where $f_{e \text{ up}} = f_e Z_{up}/L$ and $g_{up} = g Z_{up}/L$, and the lower soil layer water balance is expressed by

$$Z_{low} \frac{d\theta_{low}}{dt} = -f_{e \text{ low}} - g_{low}, \quad (14)$$

where $f_{e \text{ low}} = f_e Z_{low}/L$ and $g_{low} = g Z_{low}/L$. The scaling length L represents the drying front depth and is calculated in Eqs. (13) and (14) as if the pressure head profile in the unsaturated soil was maintained hydrostatic during the drying event, with a minimum threshold of $(Z_{up} + Z_{low})$. Under these assumptions, from the $\theta(\psi)$ constitutive relationship provided by Brooks and Corey (1966), one can obtain

$$L(t) = \max \left\{ |\psi_s| [\Theta_{up}(t)]^{-1/\eta}, Z_{up} + Z_{low} \right\}. \quad (15)$$

Equations (13) and (14) are solved numerically during the interstorm event by applying a simple explicit Euler scheme (see Orlandini, 1998).

3 Real case application

The SVATS developed in this paper is tested against rates of evaporation calculated from measurements of the Bowen

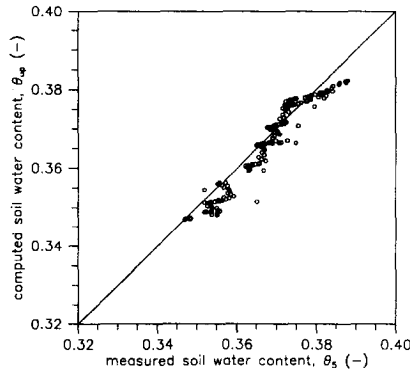


Fig. 3. Comparison between model computations of the average moisture content at the upper soil layer, θ_{up} , and TDR measurements of soil moisture content at 5 cm depth, θ_5 .

ratio and soil moisture data obtained from TDR measurements. Field data were collected by the Laboratory of Hydrology and Water Management of the University of Ghent (Belgium) and refer to a bare soil plot in the Zwalmbeek catchment. Atmospheric variables and soil moisture measurements were available for three periods of several days each among which the August 9–17, 1994, period was selected to present the capabilities of the proposed formulation. The parameter values used in the present study are reported in Table 1. Vegetation parameters (h , LAI, C , μ , ν) are set here to reproduce the surface roughness and storage capacity of the bare soil. Surface resistances ($r_{s \min}$, $r_{s \max}$) are estimated as fitting parameters on the basis of simulated and measured actual cumulative evaporation depths. Soil hydraulic properties (θ_r , θ_s , η , ψ_s , K_s) are obtained from detailed laboratory water release curve analysis, and are typical of clay soils. Structural parameters (Z_{up} , Z_{low}) are set to provide a useful representation of the near-surface soil dynamics for both interstorm and storm events (Orlandini et al., 1996).

The computed average moisture content time series for the upper soil layer ($Z_{up} = 0.10$ m), θ_{up} , are compared with TDR soil moisture measurements at 5 cm depth below the land surface in Fig. 2, where the ground level precipitation

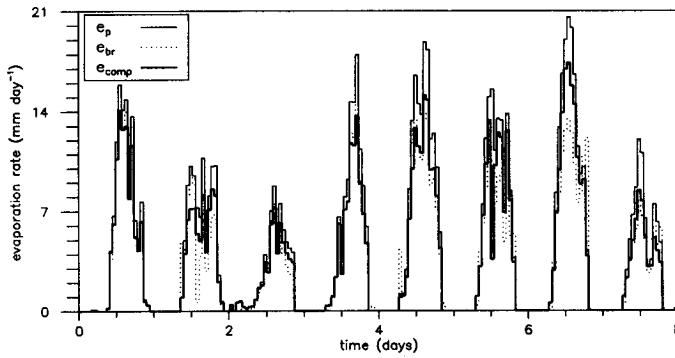


Fig. 4. Comparison between time series of computed actual evaporation rates, e_{comp} , and actual evaporation rates calculated from Bowen ratio measurements, e_{br} .

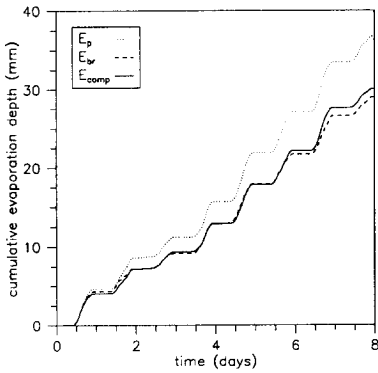


Fig. 5. Comparison between model computations of actual cumulative evaporation depth, E_{comp} , and actual cumulative evaporation depths calculated from Bowen ratio measurements, E_{br} .

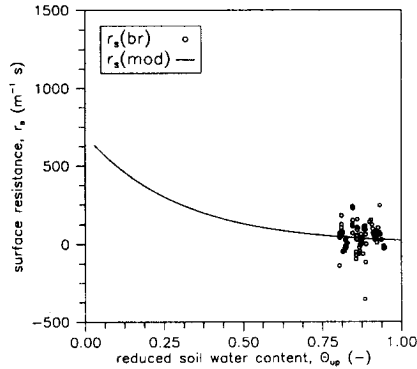


Fig. 6. Comparison between values of surface resistance obtained from field measurements through the Eq. (18), $r_s(br)$, and those obtained from the model relationship (11), $r_s(mod)$.

p_n is also reported to allow the distinction between storm and interstorm events in the simulation period. The agreement between simulated and observed data is also shown in Fig. 3, in the form of a scatter plot. Hourly mean evaporation was calculated by applying the energy balance method where the Bowen ratio concept was incorporated. Since the sensible-heat term Q_h of the energy balance equation is difficult to measure, it is commonly related to the energy used in evaporation Q_e as $Q_h = R Q_e$, where the Bowen ratio R is expressed as

$$R = \frac{c_p p_a}{0.622 L_e} \frac{T(z) - T(z_o + d)}{\epsilon(z) - \epsilon(z_o + d)}, \quad (16)$$

z being the screen height (Bras, 1990). If we apply the Bowen ratio concept, the latent-heat flux can be derived directly from the energy balance equation as follows:

$$\rho_w L_e e_{br} = \frac{Q_n - Q_g}{1 + R}, \quad (17)$$

where e_{br} is the rate of evaporation calculated from measurements of the Bowen ratio R . The computed actual evaporation time series ($e_{comp} = e_i + f_e$) is compared with the evaporation obtained from Bowen ratio measurements (e_{br}) in Fig. 4, in which the atmospheric evaporative demand (e_p)

is also reported. Cumulative evaporation depths are plotted in Fig. 5, where E_p , E_{br} , and E_{comp} denote the integrals of the e_p , e_{br} , and e_{comp} evaporation rates, respectively.

By using the Penman-Monteith equation (1) with estimation of the energy budget, the surface resistance to water vapour transfer can be obtained. On rearrangement of Eq. (1), the surface resistance r_s is given by

$$r_s = \left(\frac{\Delta R}{\gamma} - 1 \right) r_a + \frac{\rho_a c_p}{\gamma(Q_n - Q_g)} [\epsilon_s(z) - \epsilon(z)] (1 + R). \quad (18)$$

Values of surface resistance restricted to those time intervals of the simulation period in which (1) $e_p > 0$ (daylight-time intervals), (2) $p = 0$ (interstorm time intervals), and (3) the actual exfiltration rate f_e is not limited by the exfiltration capacity f_{e*} , are calculated through Eq. (18), namely $r_s(br)$, and are plotted in Fig. 6 together with values obtained from the model relationship (11), namely $r_s(mod)$.

4 Discussion

The comparison of simultaneously simulated evaporation fluxes and topsoil moisture contents with measured data were

satisfactory (Figs. 3 and 5). It is possible that the overestimation of actual evaporation in Fig. 5 is due to neglecting physical effects such as thermally induced downward gradients of vapour. It could also simply be model error induced by the many mathematical assumptions in the proposed formulation. It should also be noted that the available measurements referred to a particular field situation in which high degrees of topsoil saturation are maintained during the entire event. This appeared clearly in Fig. 6, where the recalculated values of surface resistance to water vapour transfer $r_s(\text{br})$ were interpreted by the model relationship (11) for a restricted range of the degree of soil saturation ($\Theta_{\text{up}} > 0.75$). Although a more comprehensive model validation is needed, especially to test the roles of surface resistance and exfiltration capacity in extreme soil drying conditions, the results obtained in the present work suffice to warrant a reliable model behaviour under humid topsoil conditions, such as those normally offered by the land surface during short interstorm periods. This is important to improve the simulation of land surface dynamics in response to sequences of storms with short interstorms, on one hand, and encourages the progress of the work for improving long-term interstorm simulations, on the other hand.

Acknowledgements. Luc Debruyckere (Laboratory of Hydrology and Water Management, University of Ghent, Belgium) is gratefully acknowledged for providing the field data used in this study. The author thanks the anonymous referees for comments that led to improvements in the manuscript.

References

- Black, T. A., Gardner, W. R., and Thurtell, G. W., The prediction of evaporation, drainage, and soil water storage for a bare soil, *Soil Sci. Soc. Amer. Proc.*, 33(5), 655–660, 1969.
- Bras, R. L., *Hydrology: An Introduction to Hydrologic Science*, Addison-Wesley, Reading, MA, 1990.
- Brooks, R. H. and Corey, A. T., Properties of porous media affecting fluid flow, *J. Irrig. Drain. Div. Am. Soc. Civ. Eng.*, 2, 61–88, 1966.
- Camillo, P. J., Gurney, R. J., and Schmutge, T. J., A soil and atmospheric boundary layer model for evaporation and soil moisture studies, *Water Resour. Res.*, 19(2), 371–380, 1983.
- Daamen, C. C. and Simmonds, L. P., Measurement of evaporation from bare soil and its estimation using surface resistance, *Water Resour. Res.*, 32(5), 1393–1402, 1996.
- Dickinson, R. E., Henderson-Sellers, A., and Kennedy, P. J., Biosphere-Atmosphere Transfer Scheme (BATS) Version 1e as coupled to the NCAR Community Climate Model, Tech. Note TM-387+STR, Natl. Cent. for Atmos. Res., Boulder, Colo., 1993.
- Eagleson, P. S., Climate, soil, and vegetation, 3. A simplified model of soil moisture movement in the liquid phase, *Water Resour. Res.*, 14(5), 722–730, 1978.
- Famiglietti, J. S. and Wood, E. F., Multiscale modeling of spatially variable water and energy balance processes, *Water Resour. Res.*, 30(11), 3061–3078, 1994.
- Flerchinger, G. N., Hanson, C. L., and Wight, J. R., Modeling evaporation and surface energy budgets across a watershed, *Water Resour. Res.*, 32(8), 2539–2548, 1996.
- Gardner, H. R., Prediction of evaporation from homogeneous soil based on the flow equation, *Soil Sci. Soc. Amer. Proc.*, 37, 513–516, 1973.
- Gardner, H. R., Prediction of water loss from a fallow field soil based on soil water flow theory, *Soil Sci. Soc. Amer. Proc.*, 38, 379–382, 1974.
- Gardner, H. R. and Gardner, W. R., Relation of water application to evaporation and storage of soil water, *Soil Sci. Soc. Amer. Proc.*, 33(3), 192–196, 1969.
- Gardner, W. R., Approximate solution of a non-steady-state drainage problem, *Soil Sci. Soc. Amer. Proc.*, 26, 129–132, 1962.
- Gardner, W. R. and Hillel, D. I., The relation of external evaporative conditions to the drying of soils, *J. Geophys. Res.*, 67(11), 4319–4325, 1962.
- Green, W. H. and Ampt, G. A., Studies on soil physics, I, Flow of air and water through soils, *J. Agric. Sci.*, 4, 1–24, 1911.
- Higuchi, M., Numerical simulation of soil water flow during drying in a non-homogeneous soil, *J. Hydrol.*, 71, 303–334, 1984.
- Mahfouf, J. F. and Noilhan, J., Comparative studies of various formulations of evaporation from bare soil using in situ data, *J. Appl. Meteorol.*, 30, 1354–1365, 1991.
- Massman, J., Water storage of a forest foliage: A general model, *Water Resour. Res.*, 5(1), 210–216, 1980.
- Milly, P. C. D., Moisture and heat transport in hysteretic, inhomogeneous porous media: A matric head-based formulation and a numerical model, *Water Resour. Res.*, 18(3), 489–498, 1982.
- Milly, P. C. D., An event-based simulation model of moisture and energy fluxes at a bare soil surface, *Water Resour. Res.*, 22(12), 1680–1692, 1986.
- Orlandini, S., A two-layer model of near-surface soil drying for time-continuous hydrologic simulations, *J. Hydrol. Engrg. Am. Soc. Civ. Eng.*, In press, 1998.
- Orlandini, S., Mancini, M., Paniconi, C., and Rosso, R., Local contributions to infiltration excess runoff for a conceptual catchment scale model, *Water Resour. Res.*, 32(7), 2003–2012, 1996.
- Passerat de Silans, A., Bruckler, L., Thony, J. L., and Vauclin, M., Numerical modeling of coupled heat and water flows during drying in a stratified bare soil: Comparison with field observations, *J. Hydrol.*, 105, 109–138, 1989.
- Philip, J. R. and de Vries, D. A., Moisture movement in porous materials under temperature gradients, *Eos Trans. AGU.*, 38(2), 222–232, 1957.
- Prill, R. C., Johnson, A. I., and Morris, D. A., Specific yield-laboratory experiments showing the effect of time on column drainage, Supply Paper 1662-B, U. S. Geological Survey, 1965.
- Richards, L. A., Gardner, W. R., and Ogata, G., Physical processes determining water loss from soil, *Soil Sci. Soc. Amer. Proc.*, 20, 310–314, 1956.
- Rutter, A. J. and Morton, A. J., A predictive model of rainfall interception in forest, III, Sensitivity of the model to stand parameters and meteorological variables, *J. Appl. Ecol.*, 14, 567–588, 1977.
- Salvucci, G. D., Soil and moisture independent estimation of stage-two evaporation from potential evaporation and albedo or surface temperature, *Water Resour. Res.*, 33(1), 111–122, 1997.
- Sellers, P. J., Mintz, Y., Sud, Y. C., and Dalcher, A., A simple biosphere model (SiB) for use within general circulation models, *J. Atmos. Sci.*, 43(6), 505–531, 1986.
- Sophocleous, M., Analysis of water and heat flow in unsaturated-saturated porous media, *Water Resour. Res.*, 15(5), 1195–1206, 1979.
- van Bavel, C. H. M. and Hillel, D. I., Calculating potential and actual evaporation from bare soil surface by simulation of concurrent flow of water and heat, *Agric. Meteorol.*, 17, 453–476, 1976.
- Wigmosta, M. S., Vail, L. W., and Lettenmaier, D. P., A distributed hydrology-vegetation model for complex terrain, *Water Resour. Res.*, 30(6), 1665–1679, 1994.
- Witono, H. and Bruckler, L., Use of remotely sensed soil moisture content as boundary conditions in soil-atmosphere water transport modeling, 1, Field validation of a water flow model, *Water Resour. Res.*, 25(12), 2423–2435, 1989.
- Youngs, E. G., The drainage of liquids from porous materials, *J. Geophys. Res.*, 65(12), 4025–4030, 1960.